Journal of
Nanoscience and Nanotechnology
Vol.10, 6136–6143, 2010

Pentagonal Nanorods and Nanoparticles with Mismatched Shell Layers

L. M. Dorogin[1], S. Vlassov[1], A. L. Kolesnikova[2], I. Kink[1], R. Lõhmus[1], and A. E. Romanov[1,3,*]

[1] *Institute of Physics, University of Tartu 51014, Tartu, Estonia*

[2] *Institute of Problems of Mechanical Engineering 199178, St. Petersburg, Russia*

[3] *Ioffe Physico-Technical Institute 194021, St. Petersburg, Russia*

Nano-scale rods and particles having the axes of fivefold symmetry, i.e., pentagonal nanorods and nanoparticles, are theoretically and experimentally investigated. Such objects possess elastic strains and mechanical stresses. In the present research a new mechanism of stress relaxation in nanorods and nanoparticles is considered. The mechanism is implemented by a formation of a surface layer with crystal lattice mismatch. The elastic fields and energies for nanorods and nanoparticles with the mismatched layers are calculated in the framework of the disclination model. The optimal mismatch parameter giving the maximal energy release is determined. The threshold radius as the minimal radius of nanorods or nanoparticles for which the formation of the layer is energetically favorable, is found. The threshold radius is approximately 10 nm for nanoparticle and 100 nm for nanorod of typical FCC metal.

Keywords: Pentagonal Nanorod, Icosahedral Nanoparticle, Mismatch Shell, Disclination.

RESEARCH ARTICLE

1. INTRODUCTION

Micro- and nano-size crystals with pentagonal symmetry are under investigation for more than five decades. They were first observed for pure metals with FCC crystal structure such as Cu, Ag, Au, but later were found for other materials, e.g., AgBr, Si, Ge, BN, TiCN etc. For detailed and comprehensive survey of the discovery of pentagonal crystals and particles including historical remarks please refer to review articles.[1–3] Pentagonal crystals and particles can be processed via physical or chemical vapor deposition on various substrates; homogeneous nucleation in inert gas atmosphere; electrodeposition; growth from melt; metal colloid precipitation, sol–gel-techniques, and even precipitation from solid solutions.[1] As the most recent experimental results on pentagonal objects observation with characteristic nano-scale dimensions we can refer to Refs. [3–7]. For example, Hofmeister in Ref. [4] studied the structure of silver pentagonal nanorods (PNRs), whereas Koga et al.[5] showed a large fraction pentagonal nanoparticles (PNPs) (decahedral and icosahedral shape) of gold against usual FCC morphology.

Rods and particles with pentagonal symmetry are also called multiply-twinned (fivefold twinned) crystalline objects.[1–3,8] This is due to the fact that their internal crystalline structure comprises from the regions separated by so-called twin boundaries providing characteristic external shape of the rods and particles. The magnitude of the twining angle in FCC crystals, which is 70.53° and is very close to $2\pi/5$, causes the possibility of the formation of twinned regions arranged about the axes of fivefold symmetry.

It is well-known that PNRs and PNPs and their larger micrometer-size relatives have internal elastic strains with corresponding mechanical stresses.[2,3] As a result of internal straining PNRs and PNPs possess stored elastic energy proportional to the volume of the PNR (or PNP). This energy can be diminished in the course of relaxation processes in PNRs (PNPs) accompanied by the formation of various defects, e.g., dislocations, disclinations, pores etc.[2,9] On the other hand it also known that physical properties of small nano-size particles can be essentially modified by the formation of a shell (or coat) layer covering the surface of a nanoobject, see for example Refs. [3, 10, 11]. Therefore the question arises how such covering layers can modify the onset of mechanical relaxation processes in nano-size particles and rods.

In the present study we propose and prove that the formation of a shell layer with crystal lattice mismatch with respect to the core region of PNRs or PNPs can diminish

*Author to whom correspondence should be addressed.

the internal energy of these nano-objects, and thus cab serve as another (alternative) way of mechanical stress relaxation.

2. APPLICATION AND PREPARATION OF SHAPE-CONTROLLED NANOPARTICLES

Shape control during the synthesis is essential for development of optimal metallic nanostructures for specific applications, such as biosensors, imaging, photothermal therapy, and photonic devices. In particular, surfaces enhanced Raman spectroscopy (SERS) using polyhedral gold nanocrystals could prove an effective tool for detecting analytes at extremely low concentrations. Similar polyhedral synthesis approaches of other face-centered cubic metals (Pd, Pt, Ni, etc.) are also in progress in order to study various surface and shape dependent catalytic reactions.

As it was already mentioned in Introduction, there exist a number of experimental techniques used to produce PNRs and PNPs. Among them there are: colloidal chemistry methods,[7, 10, 12] electrolysis[1, 6] and vapor phase deposition.[1, 2, 13] Colloidal methods are the oldest and simplest methods for preparation of metal nanoparticles. All colloidal methods rely on well established wet chemistry processes in which solutions of different ions are mixed under controlled conditions (temperature etc.) to form insoluble precipitates. For example, a common method of preparation of gold nanoparticles is based on reduction of Au ions in a mixture of tetrachloroauric(III) acid hydrate ($[HAuCl_4]\cdot H_2O$) and trisodium citrate. By reducing the $HAuCl_4$ with trisodium citrate, stabilized Au nanoparticles, which bear the negative charge of the citrate ions, are obtained.[12] The average size of the obtained nanoparticles can be controlled during reaction by temperature, steering, or chemically by adding chemicals like $NaBH_4$ and can range from several nm to tens and hundreds of nm.[12] Moreover, the shape of nanoparticles can also be adjusted by varying the reaction conditions.[7]

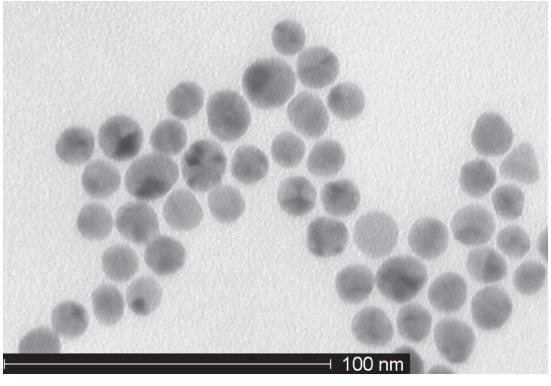

Fig. 1. Golden nanoparticles obtained by chemical reaction root. Reprinted with permission from [12], K. Mougin et al., *Private Communications* (**2008**). © 2008.

Nanoparticles obtained by a colloidal method are shown in Figure 1. It can be clearly seen that some fraction of the nanoparticles have pentagonal structure.

Not only single-component, but also multi-component nanostructures like metals combined in core/shell configurations can be synthesized in a simple colloidal chemistry reactions. Such structures attract much attention from both the experimental and theoretical points of view, possessing new physical and chemical properties not observed in individual components. Examples of multi-component nanostructures synthesis can be found in Refs. [10, 14]. For preparation of bimetallic Au–Pt nanoparticles the following scheme was used: 0, 4 g poly(N-vinyl-2-pyrrolidone) (PVP) was dissolved in 50 ml of 1,2-ethylenediol (EG) under vigorous stirring, heating in reflux until the desired temperature was reached (working temperature ranged from 100 °C to 190 °C in increments of 10 °C). Then 0.1 mM aqueous solution of the metal precursor was added to the EG-PVP solution with continuous agitation for three hours in reflux. After complete dissolution of PVP in EG, 2 ml of an aqueous solution of H_2PtCl_6 (0.05 M) was added to the EG-EVP solution. One minute after a change in color of the solution from yellow to dark brown was observed, 1 ml of an aqueous solution of $HAuCl_4$ (0.1 M) was added to the system. The basic polyol method was followed to obtain bimetallic NPs passivated with PVP.

Nanorods can be also obtained by a chemical way. Silver nanorods made via a chemical reaction were investigated by Chen et al.[15]

3. THEORETICAL BACKGROUND

A number of models explaining various aspects of formation mechanisms and physical properties of elongated pentagonal nanorods and pentagonal nanoparticles exist, e.g., Refs. [2, 3, 16–19] Among these models, the disclination approach[2, 16, 17] presents a natural way for the quantitative analysis of non-uniform crystal lattice distortions in PNPs and PNRs.

3.1. Disclination Model of Pentagonal Nanorod

Figure 2 presents the disclination model for a PNR. The crystal geometry of a PNR includes five FCC monocrystalline regions divided by five twin boundaries.[2, 16] Lateral faces of this multiple-twinned PNR are crystallographic planes of {100}-type, whereas cup faces are of {111}-type (Fig. 2(a)). The axis of fivefold symmetry is parallel to the ⟨110⟩-type direction. Because of the FCC crystal geometry there exists a small angular gap ω preventing the formation of completely connected and undistorted PNR (Figs. 2(b, c)). This angular gap can be eliminated by mutual rotation of the gap faces with the introduction of the positive wedge disclination of the strength ω along the PNR axis. The disclination strength ω is related to

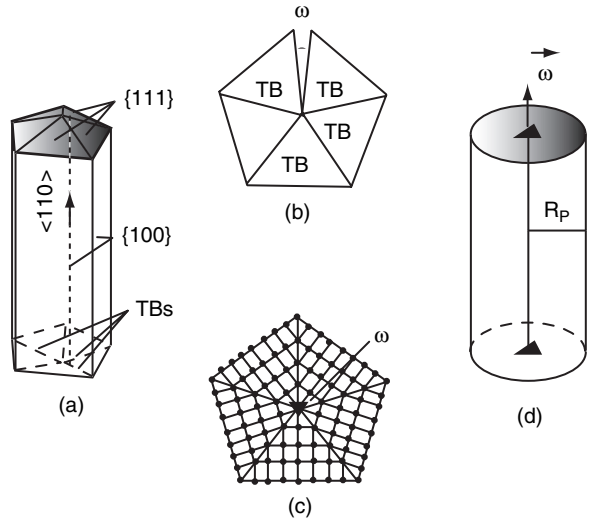

Fig. 2. Disclination model for pentagonal nanorods (PNRs). (a) PNR with internal twin boundaries, (b) angular gap ω in a PNR, (c) twinned crystal lattice of PNR, (d) PNR modeled as cylinder of radius R_P having positive wedge disclination of strength ω.

the twinning angle α_{twin} in FCC lattice (see, for example, Ref. [2]):

$$\omega = 2\pi - 5\alpha_{\text{twin}} = 2\pi - 10\sin^{-1}\left(\frac{\sqrt{3}}{3}\right) \approx 7^0 20' \quad (1)$$

The presence of disclination leads to elastic distortions of the crystal lattice in the bulk of PNR. In the continuum mechanics model, which is suitable for the calculation of elastic fields and energies, a PNR can be described as an elastic cylinder of radius R_P with coaxial positive wedge disclination as shown in Figure 2(d). For experimentally observed PNRs R_P varies from 10 nm to 1 μm.[1–3, 6, 20]

Non-zero components of wedge disclination stress tensor in cylindrical coordinate system (r, φ, z) associated with PNR axis are:[21]

$$\sigma_{rr} = \frac{\omega G}{2\pi(1-\nu)}\ln\left(\frac{r}{R_P}\right) \quad (2a)$$

$$\sigma_{\varphi\varphi} = \frac{\omega G}{2\pi(1-\nu)}\left[1+\ln\left(\frac{r}{R_P}\right)\right] \quad (2b)$$

$$\sigma_{zz} = \frac{\omega G\nu}{2\pi(1-\nu)}\left[1+2\ln\left(\frac{r}{R_P}\right)\right] \quad (2c)$$

where G is a shear modulus, ν is Poison's ratio.

The elastic energy of disclination per unit length of PNR is:[21]

$$E_\omega = \frac{\omega^2 G R_P^2}{16\pi(1-\nu)} \quad (3)$$

The energy given by Eq. (3) rapidly increases with the cylinder radius. Therefore the development of relaxation processes, which can diminish the stored energy, must be expected. It was theoretically proposed[9, 22] and proved experimentally[2, 3, 6] that mechanical stresses associated with the aforementioned distortions can relax via formation of crystal lattice defects: dislocations, disclinations, pores etc. For example, in Ref. [22] it was shown that the mechanical stresses in PNRs can be diminished by formation of dislocation loops in PNR cross-section.

3.2. Disclination Model of Pentagonal Nanoparticle

A similar approach can be applied to the modeling of PNP internal structure as it is shown in Figure 3. PNP crystal geometry includes FCC monocrystalline regions divided by twin boundaries confined by 20 tetrahedrons. Due to the FCC crystal geometry an angular gap exists (Fig. 3(a)). The gap is of more complicated shape than in the case of PNR. This gap can be closed by introducing 6 positive wedge disclinations with strength ω like given in Figure 3(b). Continuum mechanics model of PNP represents as an elastic spheroid of radius R_P with continuously distributed cones of taken out material with infinitesimal solid angle $d\beta$ that constitutes so-called Marks-Yoffe disclination (Figs. 3(c, d)).[17] The Marks-Yoffe disclination has eigenstrain components $\varepsilon^*_{\theta\theta} = \varepsilon^*_{\varphi\varphi}$ of magnitude χ:

$$\chi = \frac{3}{2\pi}\omega \approx 0.0613 \quad (4)$$

Non-zero stress components of such disclination in spherical coordinate system (r, θ, φ) associated with PNP center are:[17]

$$\sigma_{rr} = \frac{4\chi G(1+\nu)}{3(1-\nu)}\ln\left(\frac{r}{R_P}\right) \quad (5a)$$

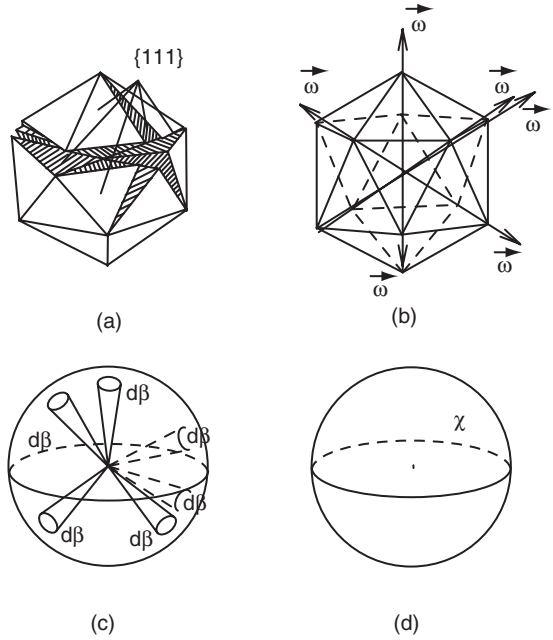

Fig. 3. Disclination model for pentagonal nanoparticles (PNPs): (a) PNP with solid angle deficiency, (b) PNP with 6 wedge disclinations of strength ω, (c) PNP with infinitesimal solid cones $d\beta$, (d) PNP modeled as spheroid with eigenstrain components $\varepsilon^*_{\theta\theta} = \varepsilon^*_{\varphi\varphi}$ of magnitude χ.

RESEARCH ARTICLE

$$\sigma_{\theta\theta} = \sigma_{\varphi\varphi} = \frac{2\chi G(1+\nu)}{3(1-\nu)}\left[1+2\ln\left(\frac{r}{R_P}\right)\right] \quad (5b)$$

The elastic energy of disclinated PNP is:[17]

$$E_\chi = \frac{8\pi\chi^2 G(1+\nu)R_P^3}{27(1-\nu)} \quad (6)$$

4. MODELING OF MISMATCHED SHELL LAYER FORMATION IN PENTAGONAL NANOROD

4.1. Energy of Pentagonal Nanorod with Mismatched Shell Layer

The model for an uniform PNR without shell layer has been described in 2.1 and is depicted in Figure 4(a). Figure 4(a) represents the initial state PNR which is normally observed. Now let us consider a non-uniform PNR consisting of two phases with different crystal lattice parameters and elastic modules. In the final state (Fig. 4(b)) the PNR is covered by layer with crystal lattice mismatch.

The elasticity problem for non-uniform PNR having a positive wedge disclination ω and different elastic modules G_1, ν_1, G_2, ν_2 as described in Figure 4, can be solved analytically. The obtained expressions for mechanical stresses of the non-uniform PNR are cumbersome functions of problem parameters $\sigma_{ij} = \sigma_{ij}(G_1, G_2, \nu_1, \nu_2, \omega, \varepsilon^*, t, R_c)$, where t is a ratio of the core radius R_c: $t = R_c/R_s$ and shell radius R_s. We provide these expressions elsewhere.[23] The lattice misfit parameter ε^* is defined as

$$\varepsilon^* = \frac{a_{core} - a_{shell}}{a_{shell}} \quad (7)$$

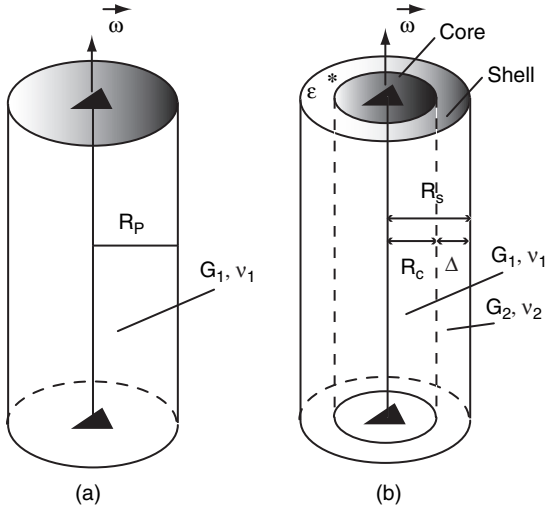

Fig. 4. Formation of shell layer with crystal lattice mismatch in pentagonal nanorods (PNRs): (a) PNR without mismatched shell layer, (b) PNR with mismatched shell layer. G_1, ν_1, G_2, ν_2 are the shear modules and Poisson's ratios of the core and shell correspondingly; R_c is a core radius; R_s is a shell radius, and ε^* is a lattice misfit parameter.

where a_{core} and a_{shell} are the lattice parameters of the core and shell. In order to investigate the behavior of the PNR covered with a shell we have solved an elasticity boundary value problem for two-phase cylinder with crystal mismatched layer.

The analysis shows that the stress components of the PNR change sign with the radius, so in the surface region of the PNR a tensile stress takes place and in the core region there is a compressive stress. Therefore we suppose that the tensile stress in the surface region of PNR can be diminished by increasing the crystal lattice constant in that region. That corresponds to the negative misfit parameters ε^*.

Total elastic energy of PNR with mismatched layer was found consisting of three terms:

$$E_{CP(\omega)} = E_\omega + E_{\varepsilon^*} + E_{\omega-\varepsilon^*} \quad (8)$$

where E_ω is the energy of two-phase cylinder with disclination:

$$\begin{aligned}
E_\omega = {} & \frac{\omega^2 R_s^2}{16\pi(1-\nu_1)(1-\nu_2)D} \\
& \cdot\{G_1^3(1+\nu_1)(1-\nu_2)t^4(2\nu_2t^2-t^2-1) - G_1^2G_2t^2 \\
& \times[-3t^4+4t^2\ln^2(t) - (1+\nu_1)\nu_2t^2 \\
& \times(-5t^2+8\ln^2(t)+2\nu_1(t^2-4\ln^2(t)-1)+5) \\
& +t^2-\nu_2^2(t^2-1)(4\nu_1t^2+t^2-1) \\
& +\nu_1(t^4-t^2+\nu_1(t^4-4t^2\ln^2(t)-1))+2] \\
& +G_2^3(1-\nu_1)(1+\nu_2)(1-2\nu_1)(t^2-1) \\
& \times((t^2-1)^2-4t^2\ln^2(t)) - G_2^2G_1 \\
& \times[3t^6-5t^4+4t^2(1-2t^2)\ln^2(t) \\
& -\nu_1^2(1+4\nu_2)t^2((t^2-1)^2-4t^2\ln^2(t))+t^2 \\
& +\nu_1(1+\nu_2)(4t^2(3t^2-1)\ln^2(t)+2\nu_2t^2((t^2-1)^2 \\
& +4\ln^2(t)) - (t^2-1)^2(5t^2+1)) \\
& +\nu_2(-(t^2-1)^3+4t^2(t^2-1)\ln^2(t) \\
& -\nu_2t^2((t^2-1)^2+8\ln^2(t)))+1]\} \\
D = {} & G_1^2(1+\nu_1)t^2(2\nu_2t^2-t^2-1) + G_1G_2(t^2-1) \\
& \times((2-\nu_2)t^2+\nu_2+1-\nu_1t^2(1+4\nu_2)) \\
& +G_2^2(1+\nu_2)(2\nu_1-1)(t^2-1)^2
\end{aligned} \quad (9)$$

E_{ε^*} is the energy of two-phase cylinder with mismatched layer:

$$\begin{aligned}
E_{\varepsilon^*} = {} & \left(\pi\varepsilon^{*2}G_1G_2(1+\nu_1)(1+\nu_2)((3t^2+1)\right. \\
& \left.\times G_1 - 3(t^2-1)G_2)t^2\ (t^2-1)R_s^2\right)/D
\end{aligned} \quad (10)$$

and $E_{\omega-\varepsilon^*}$ is an interaction energy between the disclination and mismatched layer in PNR:

$$\begin{aligned}
E_{\omega-\varepsilon^*} = {} & \left(2\omega\varepsilon^*G_1G_2(1+\nu_1)(1+\nu_2)\right. \\
& \left.\times((G_1-G_2)t^2+G_2)\ t^2\ln(t)R_s^2\right)/D
\end{aligned} \quad (11)$$

In Eqs. (9)–(11) the energies are given per unit length of a cylinder.

4.2. Critical Conditions for Mismatched Layer Formation in Pentagonal Nanorod

Energy release after formation of the mismatching layer in PNR was defined as:

$$\Delta E^{\gamma}_{\mathrm{CP}(\omega)} = (E_{\omega} + E_{\varepsilon^*} + E_{\omega-\varepsilon^*}) - E^0_{\omega} \tag{12}$$

where E^0_{ω} is the energy of uncovered PNR with radius R_s.

The diagrams for energy release in PNR in the case of equal elastic modules ($G_1 = G_2 = G$, $\nu_1 = \nu_2 = \nu = 0.3$) are depicted on Figure 5. One can notice areas where $\Delta E_{\mathrm{CP}(\omega)} < 0$ meaning that formation of such a layer is energetically favorable. Shell layers with $\varepsilon^* > 0$ increase the total elastic energy of PNR, hence they can not relax the internal stresses in PNR. The layers with $\varepsilon^* < 0$ diminish the total elastic energy, therefore the layers with such crystal lattice mismatch parameters will relax the internal stresses in PNR. Optimal mismatch parameter $\varepsilon^*_{\mathrm{opt}}$ and radii ratio t_{opt} are defined as the parameters which give the maximum elastic energy release. For PNR they were obtained numerically: $\varepsilon^*_{\mathrm{opt}} \approx -0.01$; $t_{\mathrm{opt}} \approx 0.45$.

Let us introduce now energies of free surface and interface in core/shell PNR:

$$E_{\gamma} = \gamma S \tag{13}$$

where γ is a free surface energy density or an interface energy density and S is an area of the free surface or interface.

Assuming the energies of free surface for covered PNR and uncovered PNR being equal, the interface energy is:

$$E_{\gamma(\omega)} = 2\pi\gamma R_c \tag{14}$$

As a result with the additional interface term, the energy release yields:

$$\Delta E^{\gamma}_{\mathrm{CP}(\omega)} = (E_{\omega} + E_{\varepsilon^*} + E_{\omega-\varepsilon^*} + E_{\gamma(\omega)}) - E^0_{\omega} \tag{15}$$

The criteria for the threshold radius $\hat{R}_s$ definition can be written as following:

$$\begin{cases} \Delta E^{\gamma}_{\mathrm{CP}(\omega)} = 0 \\ \dfrac{\partial \Delta E^{\gamma}_{\mathrm{CP}(\omega)}}{\partial t} = 0 \\ t \neq 0 \end{cases} \tag{16a, b, c}$$

From these equations, for example, for Cu PNR ($\gamma = 0.625$ J/m^2, $G = 5.46 \cdot 10^{10}$ Pa, [24]) the threshold radius is $\hat{R}_s \approx 130$ nm (Fig. 6). The formation of shell layer with the mismatch parameter ε^* close to the optimal value on PNRs is energetically favorable for PNRs with $R_P > \hat{R}_s$.

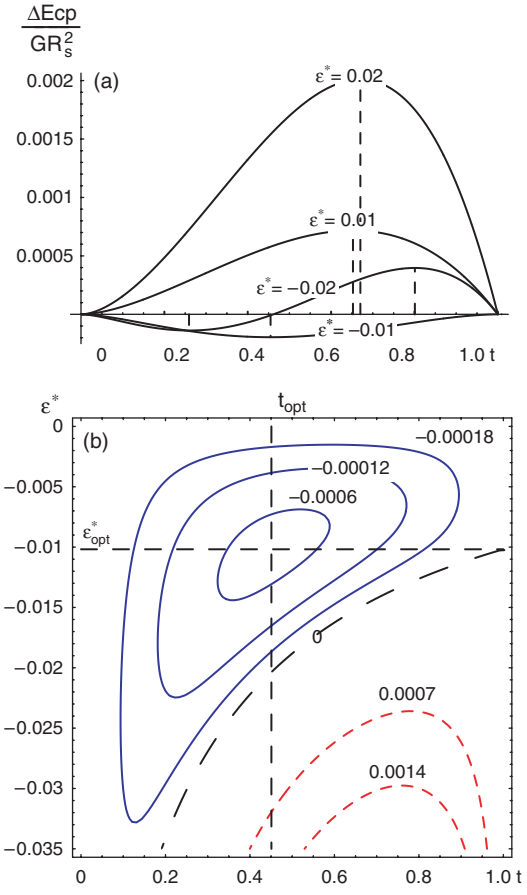

Fig. 5. Diagrams of the energy release after formation of the mismatch layer in pentagonal nanorods: (a) energy release $\Delta E_{\mathrm{CP}(\omega)}$ as function of the core/shell radii ratio t with different misfit parameters ε^*, (b) contours of the energy release $\Delta E_{\mathrm{CP}(\omega)}$ as function of t and mismatch parameter (blue contours correspond to $\Delta E_{\mathrm{CP}(\omega)} < 0$, red ones to $\Delta E_{\mathrm{CP}(\omega)} > 0$). Energy per unit length is in units GR_s^2, where G is a shear module of core and shell, R_s is a shell radius, and Poisson's ratio of core and shell $\nu = 0.3$.

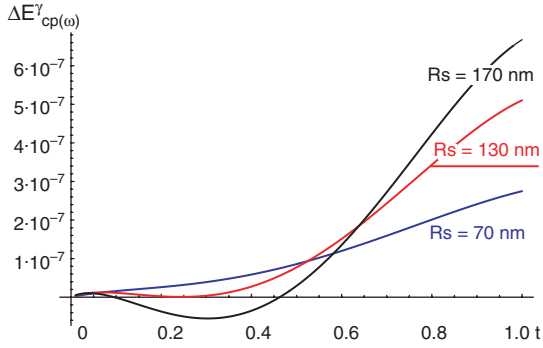

Fig. 6. Typical diagram of the energy release $\Delta E^{\gamma}_{\mathrm{CP}(\omega)}$ for covered pentagonal nanorods with the interface energy γ taken into account. For these plots $\gamma = 0.625$ Jm^{-2}, shear module of core and shell $G = 5.46 \cdot 10^{10}$ Pa, Poisson's ratio of core and shell $\nu = 0.3$, and misfit parameter $\varepsilon^* = -0.01$.

5. MODELING OF MISMATCHED SHELL LAYER FORMATION IN PENTAGONAL NANOPARTICLE

5.1. Energy of Pentagonal Nanoparticle with Mismatched Shell Layer

A similar approach can be applied to the elasticity problem for PNP. Figure 7 represents the initial and the final states of the PNP before and after mismatched shell layer formation.

The expressions for elastic fields, e.g., stresses, of the non-uniform PNP as function of its parameters are obtained: $\sigma_{ij} = \sigma_{ij}(G_1, G_2, \nu_1, \nu_2, \omega, \varepsilon^*, t, R_s)$, where t is a ratio of the core radius R_c and shell radius R_s: $t = R_c/R_s$.

The stress components of the PNP change sign with the radius, hence in the surface region of the PNP a tensile stress takes place and in the core region there is a compressive stress. The tensile stress in the surface region of PNP can be diminished by increasing the crystal lattice parameter.

In order to find the elastic fields and energy of the PNP with such lattice mismatched layer, the boundary value problems similar to that for PNR were solved.

It was found that total elastic energy of PNP with mismatched layer is:

$$E_{CP(\chi)} = E_\chi + E_{\varepsilon^*} + E_{\chi-\varepsilon^*} \tag{17}$$

where E_χ is the energy of two-phase spheroid with Marks-Yoffe disclination:

$$\begin{aligned} E_\chi = {} & (8\pi\chi^2 R_s^3)/(27(1-\nu_1)(1-\nu_2)(G_1(1+\nu_1) \\ & (-2t^3+\nu_2(4t^3-1)-1) \\ & +2G_2(1+\nu_2)(1-2\nu_1)(t^3-1))) \\ & \times\{-G_1^2(1+\nu_1)^2 t^3[-6\nu_2 t^3+2t^3+\nu_2^2(4t^3-1)+1] \\ & -2G_2^2(1+\nu_2)^2(1+\nu_1(2\nu_1-3))[(t^3-1)^2 \\ & -9t^3\ln^2(t)]+G_1G_2(1+\nu_1)(1+\nu_2) \\ & \cdot[\nu_1(-6t^6+18t^3\ln^2(t)+5t^3+\nu_2(8t^6-36t^3\ln^2(t) \\ & -9t^3+1)+1)+\nu_2(-6t^6+36t^3\ln^2(t)+7t^3-1) \\ & +4t^6-18t^3\ln^2(t)-3t^3-1]\} \end{aligned} \tag{18}$$

E_{ε^*} is the elastic energy of two-phase spheroid with mismatched layer:

$$E_{\varepsilon^*} = \frac{8\pi\varepsilon^{*2}G_1G_2(1+\nu_1)(1+\nu_2)t^3(t^3-1)R_s^3G_1(1+\nu_1)(-2t^3+\nu_2(}{4t^3-1)-1)+2G_2(1+\nu_2)(1-2\nu_1)(t^3-1)} \tag{19}$$

And $E_{\chi-\varepsilon^*}$ is interaction energy between the Marks-Yoffe disclination and mismatched layer in PNP:

$$E_{\chi-\varepsilon^*} = \frac{16\pi\chi\varepsilon^* G_1G_2(1+\nu_1)(1+\nu_2)t^3\ln(t)R_s^3}{G_1(1+\nu_1)(-2t^3+\nu_2(4t^3-1)-1)+2G_2(1+\nu_2)(1-2\nu_1)(t^3-1)} \tag{20}$$

5.2. Critical Conditions for Mismatched Layer Formation in Pentagonal Nanoparticle

Energy release $\Delta E_{CP(\chi)}$ after formation of the mismatching layer in PNP is defined as:

$$\Delta E_{CP(\chi)} = (E_\chi + E_{\varepsilon^*} + E_{\chi-\varepsilon^*}) - E_\chi^0 \tag{21}$$

where E_χ^0 is the energy of the uncovered PNP with radius R_s.

The diagrams for energy release in PNP in the case of equal elastic modules ($G_1 = G_2 = G$, $\nu_1 = \nu_2 = \nu$) are given in Figure 8. The optimal parameters ε^*_{opt} and t_{opt} at which the energy release was maximal were obtained numerically: $\varepsilon^*_{opt} \approx -0.04$ and $t_{opt} \approx 0.59$.

The interface energy term can be introduce in a manner like it was done in the Section 4.2:

$$E_{\gamma(\chi)} = 4\pi R_c^2 \tag{22}$$

Hence, with the additional interface term, the energy release for PNP yields:

$$\Delta E^\gamma_{CP(\chi)} = (E_\chi + E_{\varepsilon^*} + E_{\chi-\varepsilon^*} + E_{\gamma(\chi)}) - E_\chi^0 \tag{23}$$

For Cu PNP ($\gamma = 0.625$ J/m^2, $G = 5.46 \cdot 10^{10}$ Pa,[24]) the threshold radius obtained from Eq. (16) is $\hat{R}_s \approx 7$ nm, for Ag PNP ($\gamma = 0.780$ J/m^2, $G = 3.38 \cdot 10^{10}$ Pa,[24]) $\hat{R}_s \approx 14$ nm. The formation of shell layer with the mismatch parameter ε^* close to the optimal value is energetically favorable for PNPs with $R_P > \hat{R}_s$.

To estimate the threshold radiuses of PNR and PNP we took into account the interface energies only. In general case the surface energies of uncovered and covered PNR or PNP should be considered.

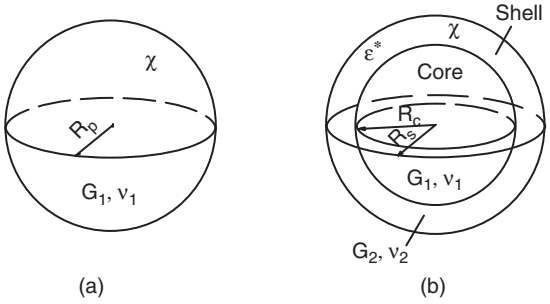

Fig. 7. Formation of shell layer with crystal lattice mismatch in pentagonal nanoparticles (PNPs): (a) PNP without mismatched shell layer, (b) PNP with mismatched shell layer. G_1, ν_1, G_2, ν_2 are the shear modules and Poisson's ratios of the core and shell correspondingly; R_c is a core radius; R_s is a shell radius and ε^* is a lattice misfit parameter.

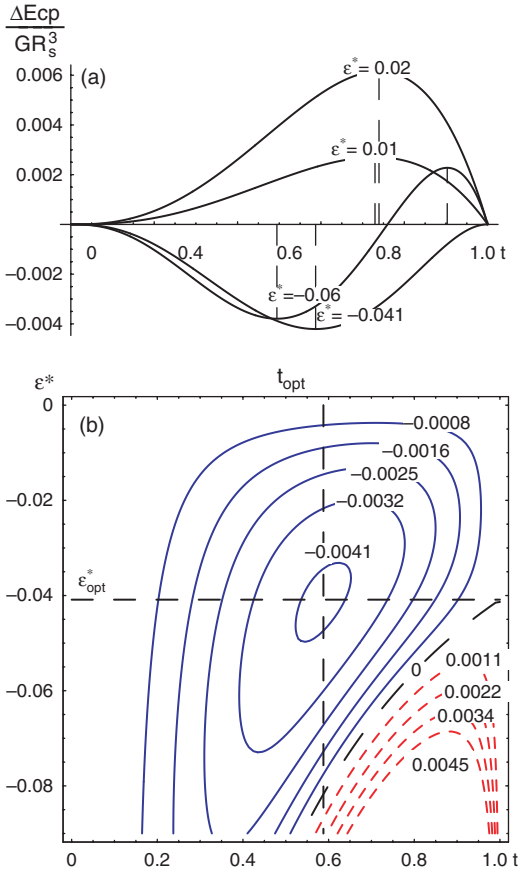

Fig. 8. Diagrams of the energy release after formation of the mismatch layer in pentagonal nanoparticles: (a) energy release $\Delta E^{\gamma}_{CP(\chi)}$ as function of the core/shell radii ratio t with different mismatch parameters, (b) contours of the energy release $\Delta E^{\gamma}_{CP(\chi)}$ as function of t and mismatch parameter (blue contours correspond to $\Delta E^{\gamma}_{CP(\chi)} < 0$, red ones to $\Delta E^{\gamma}_{CP(\chi)} > 0$). Energy is in units GR_s^3, where G is a shear module of core and shell, R_s is a shell radius, and Poisson's ratio of core and shell $\nu = 0.3$.

6. DISCUSSIONS

In our recent works[25, 26] we have proposed the initial models of core/shell formation in pentagonal nanorods and nanoparticles exploring the energy release accompanying mismatched shell formation. Pentagonal nanoparticles with core/shell configuration were prepared and investigated in Ref. [13], where copper nanoparticles were grown with silver shells. The core/shell pentagonal nanoparticles also have been studied by molecular dynamics simulation method.[27, 28] It was shown that for Cu–Ni and Cu–Pd systems[28] the location of "smaller" atoms of Cu in the core of icosahedral nanoclusters decreases the energy of the system. The Ag–Pd and Ag–Cu systems considered in Ref. [27] also confirmed that formation of shell with larger lattice parameter is energetically favorable.

In present article we have further developed our investigations started in Refs. [25, 26] and expanded the initial ideas to pentagonal nanoparticles and nanorods with nonuniform elastic properties. As a following step in the analysis of the present topic, we plan to compare the results of modeling and simulation with the experimental results for the core/shell bimetallic nanoparticles prepared by the colloidal methods. Along with high resolution electron microscopy observations, UV/VIS spectroscopy would be applied according to the method used by Seo et al. in Ref. [7], where theoretically calculated spectra of gold decahedra and icosahedra were compared with the experimental data and good agreement was reported.

7. CONCLUSIONS

On the base of our modeling and calculations we conclude that formation of a shell layer with crystal lattice mismatch can diminish the internal energy of pentagonal nanorods or pentagonal nanoparticles. This can be considered as a new mechanism of stress relaxation in pentagonal nanorods and pentagonal nanoparticles. The optimal mismatch parameter ε^*_{opt} giving the maximal energy release was determined as $\varepsilon^*_{opt} \approx -0.01$ for PNR and $\varepsilon^*_{opt} \approx -0.04$ for PNP. The threshold radius as the minimal radius of nanorods or nanoparticles for which the formation of the layer is energetically favorable was found to be approximately 10 nm for nanoparticles and 100 nm for nanorods of typical FCC metal.

Acknowledgments: The authors would like to thank Dr. K. Mougin for useful discussions on nanoparticle topics and the possibility to present her experimental micrograph for Au nanoparticles. This work was supported by the European Science Foundation project no. 1.01010337, Fanas program "Nanoparma", and Estonian Science Foundation under grants Nr. 6658 and 6537. Russian Foundation for Basic Research (projects 05-08-65503a and 07-01-00659a) is also gratefully acknowledged.

References and Notes

1. H. Hofmeister, *Cryst. Res. Technol.* 33, 3 (**1998**).
2. V. G. Gryaznov, J. Heidenreich, A. M. Kaprelov, S. A. Nepijko, A. E. Romanov, and J. Urban, *Cryst. Res. Technol.* 34, 1091 (**1999**).
3. M. J. Yacaman, J. A. Ascencio, H. B. Liu, and J. Gardea-Torresday, *J. Vac. Sci. Technol. B* 19, 1091 (**2001**).
4. H. Hofmeister, S. A. Nepijko, D. N. Ievlev, W. Schulze, and G. Ertl, *J. Cryst. Growth* 234, 773 (**2002**).
5. K. Koga and K. Sugawara, *Surf. Science* 529, 23 (**2003**).
6. I. S. Yasnikov, *Tech. Phys. Lett.* 52, 666 (**2007**).
7. D. Seo, C. I. Yoo, I. S. Chung, S. M. Park, S. Ryu, and S. Hyunjoon, *J. Phys. Chem. C* 112, 2469 (**2008**).
8. J. L. Elechiguerra, J. Reyes-Gasga, and M. J. Yacaman, *J. Mater. Chem.* 16, 3906 (**2006**).
9. V. G. Gryaznov, A. M. Kaprelov, A. E. Romanov, and I. A. Polonskii, *Phys. Stat. Sol. (b)* 167, 441 (**1991**).
10. D. I. Garcia-Gutierrez, C. E. Gutierrez-Wing, L. Giovanetti, J. M. Ramallo-Lopez, F. G. Requejo, and M. J. Yacaman, *J. Phys. Chem. B* 109, 3813 (**2005**).
11. M. Kanehara, Y. Watanabe, and T. Toshiharu, *J. Nanosci. Nanotechnol.* 9, 673 (**2009**).

RESEARCH ARTICLE

12. K. Mougin, Z. Zheng, E. Gnecco, A. Rao, and H. Haidara, *Private Communications* **(2008)**.
13. C. Langlois, D. Alloyeau, Y. Le Bouar, A. Loiseau, T. Oikawa, C. Mottetd, and C. Ricolleaua, *Faraday Discussions* 138, 375 **(2008)**.
14. J. Luo, L. Wang, D. Mott, P. N. Njoki, Y. Lin, T. He, Z. Xu, B. N. Wanjana, I.-I. S. Lim, and C.-J. Zhong, *Adv. Mater.* 20, 4342 **(2008)**.
15. H. Chen, G. Yan, Y. Hongchun, Z. Huairou, L. Libao, S. Youguo, T. Huanfang, X. Sishen, and L. Jianqi, *Micron* 35, 469 **(2004)**.
16. R. De Wit, *J. Phys. C* 5, 529 **(1972)**.
17. A. Howie and L. D. Marks, *Phil. Mag. A* 49–1, 95 **(1984)**.
18. A. S. Barnard, *J. Phys. Chem. B* 110, 24498 **(2006)**.
19. R. Könenkamp, R. C. Word, M. Dosmailov, and A. Nadarajah, *Phys. Stat. Sol. (RRL)* 1, 101 **(2007)**.
20. Y. Sun and Y. Xia, *Adv. Mater.* 16, 264 **(2004)**.
21. A. E. Romanov and V. I. Vladimirov, Dislocations in Solids, edited by F. R. N. Nabarro, North-Holland, Amsterdam **(1992)**, Vol. 9, pp. 191–402.
22. A. L. Kolesnikova and A. E. Romanov, *Tech. Phys. Lett.* 33, 886 **(2007)**.
23. L. M. Dorogin, I. Kink, A. L. Kolesnikova, and A. E. Romanov, to be published.
24. J. P. Hirth and J. Lothe, Theory of Dislocations, Willey, New-York **(1982)**.
25. A. L. Kolesnikova and A. E. Romanov, *Phys. Status Solidi (RRL)* 1, 271 **(2007)**.
26. L. M. Dorogin, A. L. Kolesnikova, and A. E. Romanov, *Tech. Phys. Lett.* 34, 779 **(2008)**.
27. F. Baletto, C. Mottet, and R. Ferrando, *Phys. Rev. B* 66, 155420 **(2002)**.
28. A. T. Kosilov, A. A. Malivanchuk, and E. A. Mikhailov, *Phys. Sol. State* 50, 1392 **(2008)**.